DOE/PC/90285--T2

SYNERGISTIC CAPTURE MECHANISMS FOR ALKALI AND SULFUR SPECIES FROM COMBUSTION

DOE/PC/90285--T2

DE92 008705

Quarterly Report No. 3

for the period March - May 1991

DOE Grant Number DE-FG22-90PC90285

Prepared by

T.W. Peterson, F.Shadman, J.O.L. Wendt and Baochun Wu
Department of Chemical Engineering,
University of Arizona,
Tucson, AZ 85721

Submitted to

Felixa Eskey,
Pittsburgh Energy Technology Center,
U.S. Department of Energy,
P.O.Box 10940
Pittsburgh, PA 15236-0940

January 10, 1992.

INTRODUCTION

Coal conversion and utilization processes, such as coal combustion, gasification and their related pollution control, have received considerable attention in recent years. Part of the reason is that the energy crisis and crude oil market instability make it necessary to seek for another fossil fuel instead. Coal is certainly an ideal one because of its huge storage on the earth and availability world wide.

There are still problems causing concern on the use of coal; for examples, efficiency and pollution. Alkali compounds cause serious fouling and slugging problems during the combustion process in pulverized coal burner and fluidized bed combustion, and will also cause corrosive problem to the furnace and the heat exchange surface as well. The fine aerosols and particles generated by the vaporizing and re-condensing of alkali compounds can also cause health problem. The recent interest of the alkali compounds control is in pressurized fluidized bed combustion (PFBC) and hot gas combined cycle, which is considered to be the most promising and efficient way of utilizing the fossil fuel like coal. The alkali compounds cause hot corrosion generally corroding the turbine blades by attacking and destroying the protective oxide layer normally present on the metal surface at high temperature, which will shorten the life time of high temperature gas turbine and increase the manufacturing expense dramatically.

Sodium and potassium exclusively represent the alkali metals in coal. In general, sodium occurs predominantly in association with organic matter in low rank lignite and subbituminous coals (Neville and Sarofim,1985). In high rank bituminous coals, sodium is found primarily in the mineral grains as halite (NaCl) and to some extent as a lattice substituent in the aluminosilicate mineral illite, a layered clay related to muscovite (Gluskoter and Ruch, 1971). In contrast, potassium is rarely observed as the halide in coals of all ranks. It was found that potassium occurs almost exclusively in the mineral illite in coals ranking from subbituminous to anthracite, but it is also present in a noncrystalline environment in lower rank subbituminous and lignite coals (Spiro et al. 1986). In selected United States coals, sodium content varies from 30 parts per million by weight to nearly one weight percent of the dry coal, while potassium varies from 30 parts per million to over two percent by weight (Harvey and Ruch.1986).

The vapor pressure of alkalies in the flue gas during the combustion is mainly determined by the form of sodium and potassium in the coal. Sodium chloride is readily vaporized above 800°C because of its low melting point and high volatility. The organically bound sodium and potassium, significant in low rank coals, is also easily volatilized during the combustion. On the other hand, it is expected that alkali associated with aluminosilicate minerals is not as readily volatilized due to its stability and low vapor pressure at combustion temperatures. Experiments showed that most of the organically bound sodium and sodium chloride were found to be volatilized in the frame, while the sodium associated with silica-rich grains was retained in the residual ash (Neville and Sarofim, 1989). Since most of the potassium in high-rank coals occurs in

the non-volatile aluminosilicate mineral illite, it is expected that little of this potassium will be vaporized during the combustion. Several ash samples from combustors, gasifiers and auxiliary equipment to determine the form of potassium after conversion of a high rank coal were analyzed (Spiro. 1986). The results showed that the potassium is present primarily as a noncrystalline aluminosilicate glass melt. The XANES features of this material were found to be identical to those obtained by pyrolysis of pure illite at 1000°C, suggesting that most of the potassium is not vaporized. It can, however, be released to the vapor phase by exchanging reaction with sodium (Jacson and Duffin. 1963). The alkali metal in ash from six different coals was explored through a 17 kw laboratory downflow pulverized coal combustor (Gallagher and Wendt et al., 1990).

The interaction of alkali with other minerals, existing in the coal, during the combustion and gasification process is quite complex and is not quite understood yet. It is considered that the form of alkali during and after combustion, as with the non-alkali mineral matter, is the result of several processes that takes place sequentially or simultaneously. Those processes include phase changes and chemical reactions, vaporization, chemical reaction in the vapor phase, nucleation of vapors and the reaction of vapors with condensed phase materials such as the mineral matter in ash and equipment surfaces (O'Gorman and Walker, 1973; Sarofim et al., 1977; Quann et al., 1982; Raask, 1985). The interactions of alkali compounds with carbon and minerals at high temperature are also investigated (Shadman and Punjak, 1989)

The gas phase reaction of alkali vapor with sulfur oxides also affects the alkali chemistry. The majority of sulfur in coal is usually associated with iron and other metals in minerals such as pyrite, marcasite and pyrrhotite (Raask, 1985). During the combustion, most of the sulfur is oxidized to gaseous SO_2 and SO_3 which then can react with other species, including alkali compounds. Alkali chlorides and oxides react rapidly with sulfur dioxide and sulfur trioxide at the temperature below 1100°C to form alkali sulfates (Reid, 1981). The thermodynamic calculations of Halstead and Raask (1969) suggest that the sulfation proceeds through a series of gas phase reactions. The alkali sulfates are also known as one of the major corrosive sources to the gas turbine. The formation of sulfates

can also occur at lower temperature without a gaseous intermediate. The formation of solid Na_2SO_4 was observed by heating coal impregnated with sodium chloride to a temperature of 475 K in air (Daybell and Pringle, 1958).

One of the major concerns is the relatively high concentration of alkali compound vapor in the gas phase. In application a low concentration is preferred for low risk of fouling and slugging and low corrosive to the equipments and heat exchange surface. In some application like PFBC and combined cycle, a extremely low concentration of alkali vapor is required. The current industrial gas turbine specification limit for alkali metal compounds in the combustion gas entering a turbine is equivalent to 0.024 ppm. An effective way for the removal of alkali vapor are by adsorption and reaction on solid sorbents. Various sorbents are tested in fixed-bed filter through which the hot flue gas passes. A series sorbents were tested under different temperature, superficial gas velocity

and residence time in order to develop a suitable sorbent for alkali sorption (Lee and Johnson, 1980). An adsorption mechanism of activated bauxite capturing the alkali chlorides is suggested with the present of water vapor, and both chemical fixation by clay minerals in the bauxite and physical adsorption are suggested without water (Lee et al., 1986). A well defined fundamental study was conducted by Luthra and Leblanc (1984) by using a thermo-gravimetric analyzer (TGA) concluding that the mechanism for alkali capture by alumina and bauxite was physical adsorption. In the present of water vapor, emathlite was found to be superior for alkali removal (Mulik et al., 1980 and 1983; Bachovchin et al., 1986). Shadman and Punjak (1988) investigated the fundamentals of alkali adsorption on kaolinite, bauxite and emathlite both experimentally and theoretically, and suggested that the alkali capturing process is not a simple physical condensation, but a complex combination of several diffusion steps and reactions. Bauxite and kaolinite react with NaCl and water vapor to form nephelite and carnegieite and release HCl. However, emathlite reacts to form albite and HCL vapor. Later works further showed the match of theoretical model with experimental data (Shadman and Uberoi, 1989). The in-situ capturing of alkali compounds by fine powder sorbents during the pulverized coal combustion is also important (Klinzing et al., 1986). Kaolinite and bauxite as in-situ additives for alkali removal were tested in our laboratory scale pulverized coal combustion system (Wendt et al., 1988).

Due to the generation of a wide variety of pollutants during coal combustion, research on the development of a multi-function sorbent for adsorbing SO_2 and alkali compounds simultaneously is ongoing at the University of Arizona. The current work

focuses on the thermodynamic behavior of the reacting system for alkali adsorption especially in gas phase. The temperature and pressure effects on sodium species and on the system are intensively investigated under the simulated flue gas composition condition. The interaction of sulfur dioxide with sodium chloride vapor and some other system elements is also explored.

EXPERIMENTAL SETUP AND PROCEDURE

EXPERIMENTAL SETUP

Several factors are considered in the design of the experimental setup. First a stable easy control source of alkali vopor is needed. Second a certain temperature range of interest must be realized. And the third a continuous weight change must be monitorable in order to obtain kinetic data from experiment. The experimental setup here is based on a thermogravimetric system. A schematic diagram of this system is given in Figure 1. It consists of four main components: a gas preparation section, a quartz reactor, an electronic microbalance to monitor alkali delivery and a movable electric furnace. A detail description of each of them is given below.

1. Gas Preparation Section

The purposes of this section is that a simulated flue gas from coal combustion furnaces is created which contains 80% of Nitrogen, 15% of carbon dioxide, 3% of oxygen and 2% of water vapor by volume. One ultra-high-pure (UHP) nitrogen cylinder of 220 cubic feet connects with two other cylinders of carbon dioxide and compressed air to form a desired mixture which will flow through a saturator to pick up some water vapor. In order to prevent water vapor condensation on the wall of its flowing tube, another UHP nitrogen is introduced after the saturator. Then the desired gas composition is obtained. To protect the balance mechanism and have a stable operation, an UHP nitrogen is used to purge the microbalance. A flow element is introduced to each cylinder for individual control of the flow rate by changing the pressure of upstream of

the element. The saturator, consisting of a gas washer and a heater, operates at 50°C, which is higher than room temperature, to be certain that it is at saturation.

2. Electronic Microbalance

A Cahn 2000 Electrobalance is used here, which can give a very sensitive in-situ monitoring of weight lose and gain during experiments. The output of the balance is as a 0-10 mv signal to a Houston Instruments strip chart recorder from the electrobalance controller. A preset chart speed allowed the weight to be monitored as a function of time. The sample itself was placed in a platinum basket that is suspended from the balance by a platinum wire. Mechanical and electronic taring of the balance allowed it to be calibrated prior to each experiment.

The Cahn 2000 balance consists of a balance beam mounted to, supported by and pivoting about the center of a taut ribbon; a torque motor coil located in a permanent magnetic field and also mounted to the taut ribbon; sample suspension fixtures; a beam position sensor system; and controls, circuitry and indicators. The principle of this balance is that the weights to be measured are applied in a downward direction from the sample side of the beam. Counterweights are applied downward from the opposite side of the beam. The forces, created by the weights, acting from both sides of the beam produce a torque about the axis of rotation. An electric current flowing in the torque motor coil also produces a torque about the axis of rotation, as does the taut ribbon. When the beam is at its horizontal reference position as detected by the beam position sensing system, and when the torque from the torque motor is equal and opposite to the

sum of the taut ribbon torque and the torques due to the forces acting from both sides of the beam, then the beam is said to be balanced. When the beam is balanced, the electric current flowing in the torque motor coil is a direct measure of the combination of forces applied from both sides of the beam and the torque from the ribbon. The current is monitored by a Cahn 2000 Controller and output to a chart recorder. during calibration, a direct readout of the weight change can be obtained from the chart recorder. The balance is designed for weight up to 2.5 grams and is sensitive to weight changes as small as 0.1 microgram.

3. Reactor System

This system consists of a quartz reactor and a high temperature furnace. A Lindberg model 54459 single zone electric furnace is used to heat the reactor. It was mounted in a vertical position with one opening at the top that allowed it to be raised so that it enclosed the lower portion of the reactor. To allow vertical motion of the furnace, four wheels were mounted on it and aligned to ride in vertical steel channel tracks. Raising and lowering of the furnace was accomplished with a hand operated winch. This configuration allowed the furnace to be preheated and then raised so that the reactor could be heated to the operating temperature in one rapid step. Likewise, lowering the furnace allowed rapid termination of the experiment at any time. The furnace temperature, with a range up to 1200°C, was controlled with a separate PID Eurotherm controller connected to a platinum/platinum-13% rhodium thermocouple. The temperatures of source and reaction zone during experiments are monitored by two chromel/alumel thermocouples.

Due to its high reactivity, sodium chloride can react with most inorganic materials at high temperature, for example pure quartz, which is most commonly used material for making high temperature reactors. Also sodium chloride is very easy to condense on just about any surface especially under 800°C. Because of those, a number of factors are under consideration in the design of the quartz reactor. First, a stable unique source is a must to maintain the sodium chloride constant concentration; Second, the source temperature must be lower than that of sorbent in order to prevent large condensation of alkali on the sorbent; Third, the temperatures of source and reaction zone are easy to control and to change within interesting temperature range. Two configurations of design are considered here. Figure 2 shows details of reactor designs. The ideal configuration is that the source be located at the bottom of the reactor while the sorbent be suspended above it. A very small amount of UHP nitrogen is introduced right above the source, between the source and sorbent, to dilute the vapor concentration of alkali compound under the saturation (Fig.2 a). The other configuration of reactor design (Fig.2 b) is that the source pan is put in the horizontal arm of the reactor heated by a separate tape heater controlled by a variable transformer. The sorbent is suspended in the main reactor assembled with the balance. The advantages of this reactor is that it is easy to control the temperature of source and sorbent separately, and it is easy to change the temperature of reaction zone.

EXPERIMENTAL PROCEDURE

Experiments will be conducted by first preparing the samples. The selected sorbent, like kaolinite and bauxite, weighing about 40 mg is pressed to become pellet of

approximately 300 micrometer thickness. The pellet then is devolatilized under nitrogen at 900°C for two hours. And then the sorbent is place in a platinum basket suspended on the balance. A typical experiment begins by placing about one gram of sodium chloride in a quartz container in the bottom or horizontal leg depending on the reactor used, then reverse the flow and let the reactor temperature of both source and sorbent reach the preset temperature and also prevent initial sodium vapor reaching the sorbent while the concentration is not uniform, waiting until everything is stabilized, turn the flow to normal and start the reaction.

THERMODYNAMIC ANALYSIS

FUNDAMENTAL OF CALCULATION

The theoretical thermodynamic properties for a chemical system can be obtained by the knowledge of chemical equilibrium compositions of the system. These properties are very useful here for designing and setting up the experiment, and are also very useful for predicting and evaluating the experimental results. There are two equivalent formulations to describe the chemical equilibrium - equilibrium constants and minimization of free energy. Comparing with each other of these two formulations, the disadvantages of the equiiibrium constants are more bookkeeping, numerical difficulties with use of components, more difficulty in testing for presence of some condensed species, and more difficult in extending the generalized method for nonideal equations of state. For these reasons, the free-energy minimization formulation is used. The condition for equilibrium may be stated in terms of any of several thermodynamic functions such as the minimization of the Gibbs free energy or Helmholtz free energy or the maximization of entropy. The function chosen mostly depends on what parameters are used for the characterization of a thermodynamic state. The Gibbs free energy is most easily minimized in as much as temperature and pressure are its natural variables. Similarly, the Helmholtz free energy is most easily minimized if the thermodynamic state is characterized by temperature and volume (or density). So as the maximization of entropy by temperature and entropy. Since the system here is characterized by temperature and pressure, the Gibbs free energy is used.

In the system here, a simulated flue gas and sodium chloride are considered. A theoretical distribution of sodium in products was calculated by assuming equilibrium conditions. This was done by using a computer program developed at NASA Lewis Research Center which has been widely accepted since 1962. The program uses the assumptions that all the gases are ideal and that the interactions among phases can be neglected. The ideal gas law is assumed to be correct even when small amounts of condensed species are present. These condensed species are assumed to occupy a negligible volume and exert a negligible pressure compared to the gaseous species.

There are large number of species in various phases were involved. Altogether 197 chemical species were considered in flue gas-NaCl system, 231 species in flue gas-NaCl-SO_2 system. There are listed in Table 1. and Table 2. respectively. In the products, species mole fraction less than 10E-8 are considered trace species, and therefore are not counted as products.

Table 3. gives the initial system feed compounds and their weight percentage.

RESULTS AND DISCUSSION

In the equilibrium calculations here, a temperature range from 700°C to 1500°C is used. A pressure range from 1 atm to 10 atm was also involved in order to explore the thermodynamic properties of the pressured systems and the possible applications in the PFBC. The gas composition used here is maintain 80% of nitrogen, 3% of oxygen, 15% of carbon and 2% of water vapor in all the calculation except in the flue gas-NaCl-

SO_2 systems where nitrogen is 79.9% and SO_2 is 0.1%, and the rests remain the same. NaCl is put inside the systems as a solid fuel.

Table 4. gives a typical result of the equilibrium calculation for the flue gas-NaCl systems. The first important result is the distribution of products, which shows what the final possible compounds are at equilibrium. Mole fraction of the products after equilibrium is another one which tells quantitatively the amount of each product in the system. The equilibrium result under selected temperatures at one atm is shown in Figure 3. The horizontal axis, the number reference to Table 3, indicates the compounds or the products of the system after equilibrium. We can see very clearly the major products of mole fraction up to the order of percentage level are CO_2, H_2O, N_2, NaCl solid, liquid and gas, O_2 and Na_2Cl_2, all of which except the last one-Na_2Cl_2 are the initial feed materials. NA2CL2 is the chemical reaction product which is not negligible especially at high temperature like above 1400°C. A more detail analysis of the compound will be discussed later. The other products have the concentration from 0.01 part per million (ppm), like $Na_2(OH)_2$ 0.013 ppm and N_2O 0.018 ppm, to few hundred ppm, like HCl 257.5 ppm and NO 310.3 ppm and NaOH 259 ppm. The gas phase composition of the same system is given in Figure 4 which indicates that the main change of the gas phase composition is caused by the phase change of the sodium chloride which mostly depends on temperature at a certain pressure, a minor contribution is from the Na_2Cl_2 and some other gases make their change in the ppm level.

Sodium species is of the most interest of this work. Figure 5 shows the distribution of sodium species in the three phases. We can see that almost all the sodium chloride will stay in the solid phase under the temperature of 1000°C. With the temperature over 1100°C, there is no solid phase. Liquid phase will be the major form of sodium species under 1200°C, and gas phase will play a significant part beside liquid phase of temperature above 1200°C. At 1500°C, as high as 35 percent of sodium species is in the gas phase, which makes up the sodium concentration inside the gas phase as high as 11 percent. The compounds and their percentage in these three phase are shown in Figure 6. The distributions of sodium species under different temperatures are given in Figure 7. The x-axis again is the sodium compounds while y-axis gives the percentages of integrated form of all the compounds left to the compound pointed on the x-axis. At 1500°C, sodium chloride in gas phase is about 27 percent of the total sodium species inside the system, Na_2Cl_2 7.5%, the other species in the vapor phase Na,NaO,NaOH and Na_2OH_2 have the concentration of 5 ppm, 0.2 ppm, 259 ppm and 0.02 ppm, the condensed phase of sodium chloride liquid makes its contribution up to about 65.4%. The fraction of each species in the vapor phase decreases rapidly with the decrease of temperature, like sodium chloride is about 9% at 1400°C, a drop of 18% from that at 1500°C, and Na_2Cl_2 has similar behavior (see also Fig.6). The total fraction of sodium species in the vapor phase is 34.8% at 1500°C, 11.5% at 1400°C, 3.1% at 1300°C, and the rest is from 0.3% at 1200°C to a few ppm at 900°C. The effect of temperature on the formation of NaCl and Na_2Cl_2 vapor is given in Figure 8. The Y-axis gives the mole percentage of NaCl and Na_2Cl_2 in the gas phase. We can see a very strong effect of temperature on both NaCl and Na_2Cl_2 concentrations in the gas phase when temperature

over 1200°C especially for temperature above 1300°C. The concentration of sodium chloride from 11% at T=1500°C drops to about 4% at T=1400°C, 1.3% at 1300°C and 0.3% at 1200°C. The concentrations drop to the order of magnitude of ppm level at temperature lower than 1100°C. Meanwhile, Na_2Cl_2 concentration changes at the same tendency, from 2.9% at 1500°C to 1.3% at 1400°C, about 0.4% at 1300°C, and 0.1 % at 1200°C and than ppms at the temperature lower than 1100°C. The results show the strong effect of temperature and also the production of significant amount of Na_2Cl_2 vapor as one of the major sodium species in the gas phase, which means the Na_2Cl_2 is not negligible. The ratio of Na_22Cl_2 to NaCl is about 13% at temperature 700°C, a linear increase with the temperature is observed in the temperature range of 700-1100°C, and a maximum of 43.67% is reached at 1100°C, and the ratio drops again almost linearly with the increase of the temperature to a value of a little more than 26% at 1500°C (see Fig. 9). Overall, a significant portion of Na_2Cl_2 is produced in this thermo-equilibrium system, which suggests that Na_2Cl_2 should be considered in the exploring of the mechanism of the sodium chloride adsorption in which most of the works done before did not consider the contribution of Na_2Cl_2.

The system behavior under the pressure is another major part of this work, which will give us some of the ideal of equilibrium properties which is not so easy to obtain by experiment and also expensive. The calculation results presented below show some very interesting points. The equilibriums at pressure 5 atm and 10 atm are given in Figure 10 and 11 respectively. Comparing with the equilibrium at 1 atm (Figure 3), the main difference is the NaCl and Na_2Cl_2 mole fractions in which the later is much higher. And

with the increase of the pressure of system, the concentrations of NaCl and Na_2Cl_2 will drop very rapidly (Figure 12 and 13), at 1500°C, NaCl concentration from 8.7 mole percent at 1 atm drops to 3.9% of mole fraction at 2 atm and 2.6% at 3 atm, and at pressure higher than that, the concentration drop tends to be slow and close to a constant of 0.8% at pressure of 10 atm and higher. It is hard to see the change of concentration of NaCl at lower temperature because of the scale difference, a scale up result at 900°C is given in Figure 14. We can see a surprising similar change pattern of concentration vs. pressure to that at high temperature of 1500°C, and in fact, this change is similar in all the temperature range except their absolute values are different with different temperature. We also notice that at pressure over 6 atm, the concentration of NaCl is very low therefore no measurements are needed for absorption of NaCl for most of PFBC-combine cycle applications.

The concentration of Na_2Cl_2 decreases with the increase of pressure as well (Figure 13), from 2.3% at 1500°C at 1 atm to 1.1% at 2 atm at the same temperature and also tends to a constant of 0.2% at 10 atm or higher. This is exactly the same change form with that of NaCl vs. pressure, which further shows the concentrations of both in the system is closely related and also shows their companionship which indicates that the mechanism of the formation of Na_2Cl_2 is proportion to NaCl concentration. Both NaCl and Na_2Cl_2 concentration drop will directly affect the composition and concentration of sodium species in the gas phase (see Figure 15). The reason for increasing of pressure resulting in a decrease of sodium species in the gas phase is that higher pressure will

make the sodium more likely to stay in the condensed phases of solid or liquid (figure 16). Condensed phases play a major part at high pressure.

The other major effect of pressure is the formation of $Na_2CO_3(2)$ at 1 and 2 atm, the product appears at temperature range of 800 to 1100°C and concentration from 0.07 ppm to about half ppm at 1 atm and from 0.07 ppm to about 1 ppm at 2 atm. At 3 atm, there is no $Na_2CO_3(2)$ at 800°C and at pressure over 4 atm, a liquid Na_2CO_3 is formed at temperature 1200°C beside $Na_2CO_3(2)$, the concentration from 0.05 ppm at 4 atm to 1.5 ppm at 10 atm.

The globe thermodynamic equilibrium calculation of the system under the pressure shows that the increase of the pressure can decrease the concentration of sodium species in the gas phase dramatically. Under the high pressure, for example pressure higher than 10 atm, and low temperature, lower than 900°C, the akali vapor concentration in the gas phase is not significant.

The presence of sulfur species in the system does not effect the sodium species in the gas phase significantly. In fact, it does not affect the formation of NaCl and Na_2Cl_2 at all (see Figure 17). The distribution of sodium species (Figure 18) is the same with or without sulfur dioxide except some of the minor change in the Na and NaO concentration, a minor reduction of them creates sodium sulfates. Because of the concentrations of Na and NaO are not significant, the formation of sodium sulfates is not significant. It is in the PPB level. The effects of temperature and pressure to the sodium

species on the system are the same to that without SO_2 as far as the major contribution of sodium species in the gas phase is NaCl and Na_2Cl_2.

CONCLUSION

The study so far includes two parts. One part is about the design of an experiment setup. The other part is about the thermodynamic equilibrium calculation and sodium species distribution. The following results are obtained:

1. The experimental system is setup and some of the experiments are underway.

2. The global thermodynamic equilibrium calculation of the system shows that temperature and pressure have a very strong effect on the sodium species concentration in the gas phase. The increase of the former will increase the sodium species concentration and the increase of the latter will decrease the concentration.

3. At pressure higher than 10 atm and temperature lower than 900°C, the formation of sodium species in the gas phase is not significant.

4. The sulfur species does not affect the sodium species in the vapor phase very much.

An extensive experimental work is planned to explore the absorption of sodium species in the gas phase and the interactions of sodium and SO_2 with calcium based sorbents and aluminum-silica based sorbents, and between sorbents themself.

REFERENCES

Daybell, G.N. and Pringle, W.J.S., Fuel, 37, 283, 1985.

Gallagher, N.B., Bool, L.E. and Wendt, J.O.L, Combus. Sci. Tech., Vol. 74, 211-221, 1990

Gluskoter, H.J. and Ruth,R.R., Fuel, 50, 65, 1971.

Halstead, W.D. and Raask, E., J. Inst. Fuel, 42, 344, 1969

Harvey, R.D. and Ruth, R.R., ACS Symposium Series, ISSN 0097-6156, 301, 1986.

Jackson, P.J., and Duffin, H C., Conf. Mechanism of Corrosion by Fuel Impurities, Marchwood U.K., Butterworth, London. 427, 1963.

Lee, S.H.D. and Johnson, I., J Eng. Power, 102,397, 1980.

Lee, S.H.D. and Henry, S.D., ANL-FE-86-7; Argonne National Labtory; Argonne, IL, 1986

Mulik, P.R. et al, DE-AC21-81MC16327, Pittsburgh, PA, 1983

Neville, M. and Sarofim, A.F., Fuel, 64(3), 384, 1985

O'Gorman, J.V. and Walker, P.L., Fuel, 52, 71, 1973

Punjak, W.A.;Uberoi, M. and Shadman, F., AICHE J., 35(7), 1989

Punjak, W.A. and Shadman, F., Energy and Fuel, 2, 702, 1988.

Rizeq, R.G., and Shadman, F., Chem, Eng, Commun, 81, 1989.

Quann, R.M. et al, Enviro. Sci. Tech., 16, 776, 1982.

Raask, E., Mineral Imperities in Coal Combustion, Hemisphere, New York, 1985.

Reid, W.T., Chemistry of Coal Utilization, New York, 1981.

Sarofim, A.F. et al, Com. Sci. and Tech., 16, 187, 1977.

Shadman, F. and Punjak, W.A., Combustion Inst., Tucson, 1986.

Spiro, C.L et al, ACS National Meeting, 34(2), 1989.

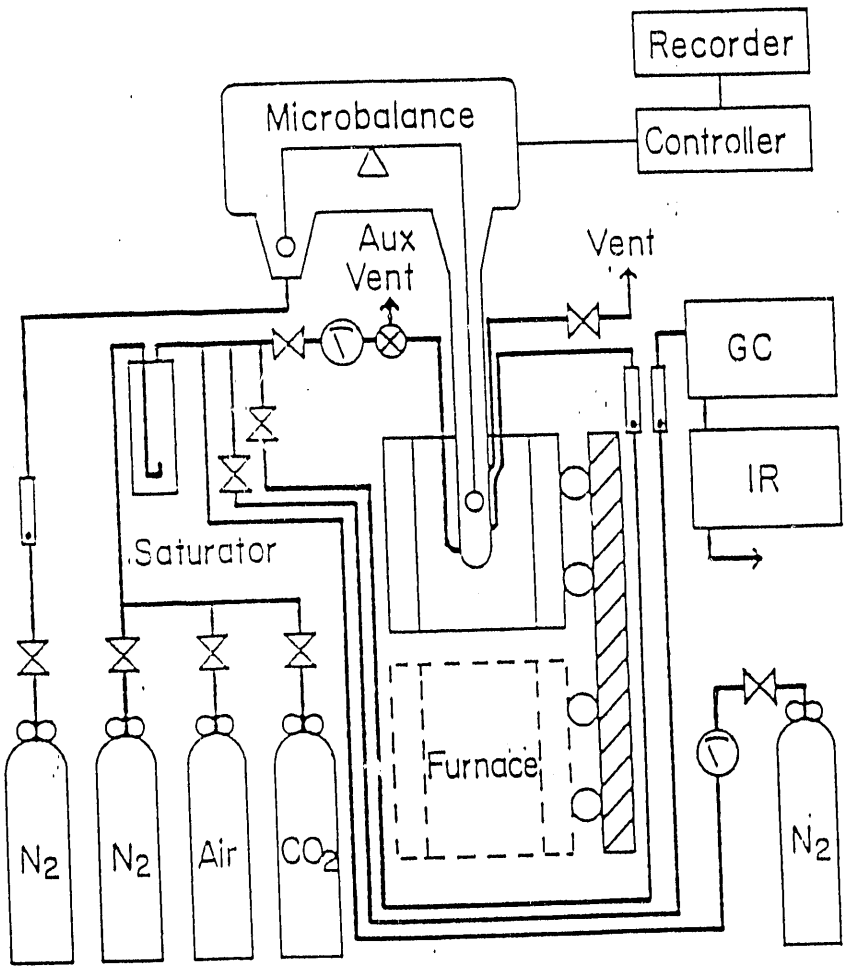

Figure 1. The Schematic of the Experiment Set Up

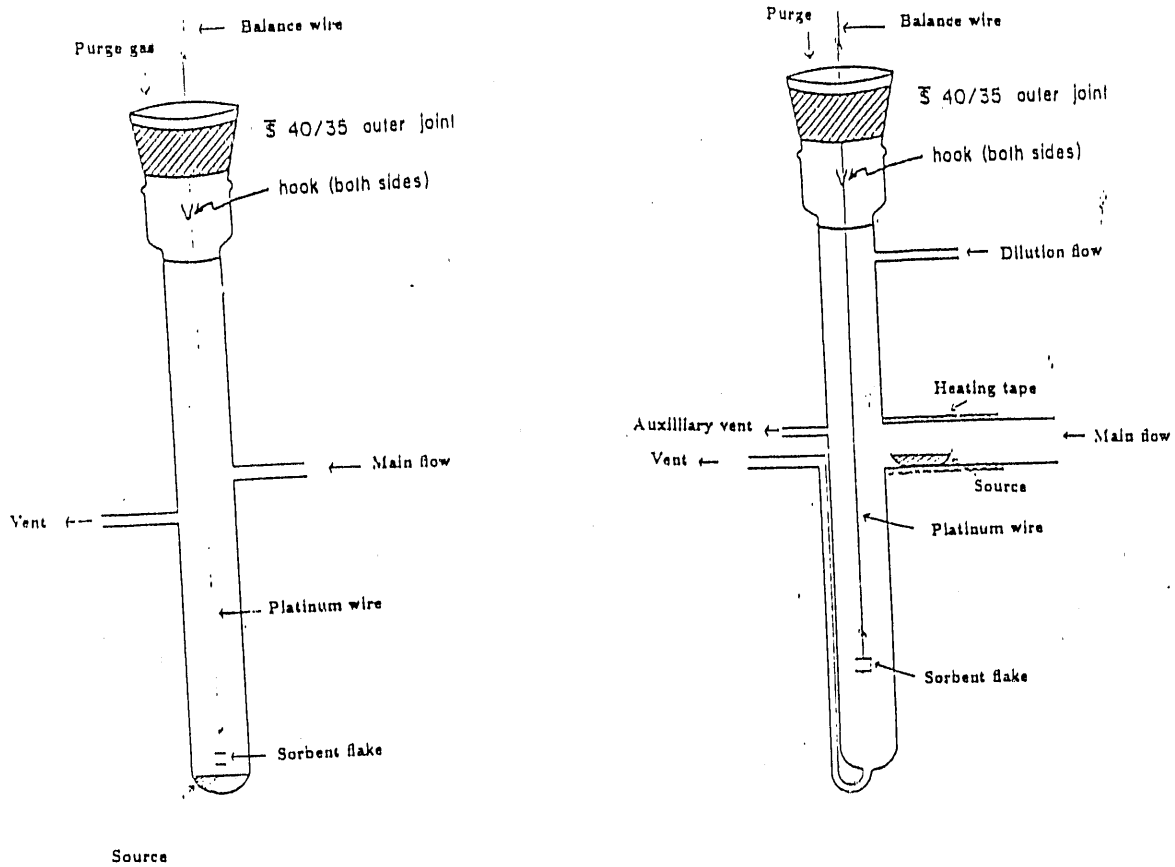

a. b.

Figure 2. The Configuration of Reactor Designs

Table 1. Mole Fractions Of Simulated Flue Gas - NaCl Equilibrium AT One Atm

Number	Compound	Mole Fraction Temperature °C 1500	1300	1100	900
1	CO	2.15E-06	6.15E-08	5.30E-10	5.52E-13
2	CO2	6.82E-02	6.69E-02	6.67E-02	6.67E-02
3	Cl	6.23E-06	2.40E-07	4.03E-09	6.76E-11
4	ClO	2.36E-08	1.31E-09	3.26E-11	9.47E-13
5	Cl2	1.46E-08	5.58E-10	1.07E-11	1.27E-12
6	HCl	2.58E-04	3.35E-05	2.80E-06	4.71E-07
7	HOCl	1.26E-08	1.44E-09	9.20E-11	1.04E-11
8	HO2	3.66E-08	8.23E-09	1.05E-09	5.34E-11
9	H2	2.69E-07	1.14E-08	1.71E-10	4.15E-13
10	H2O	2.19E-02	2.17E-02	2.17E-02	2.17E-02
11	NO	3.10E-04	9.87E-05	2.12E-05	2.30E-06
12	NO2	5.63E-07	3.89E-07	2.21E-07	9.82E-08
13	N2	5.71E-01	5.60E-01	5.59E-01	5.59E-01
14	N2O	1.84E-08	6.75E-09	1.65E-09	2.20E-10

Table 1. Continued.....

15	Na	4.57E-06	5.86E-08	1.45E-10	2.05E-15
16	NaCl	8.67E-02	8.50E-03	3.91E-04	2.21E-06
17	NaO	1.89E-07	3.49E-09	1.31E-11	3.31E-16
18	NaOH	2.59E-04	3.37E-05	1.76E-06	2.02E-09
19	Na2Cl2	2.31E-02	2.89E-03	1.71E-04	6.71E-07
20	Na2(OH)2	1.35E-08	3.81E-09	4.00E-10	1.03E-13
21	O	4.89E-07	1.96E-08	2.74E-10	5.91E-13
22	OH	1.94E-05	2.49E-06	1.61E-07	3.14E-09
23	O2	1.86E-02	1.83E-02	1.83E-02	1.83E-02
24	NaCL(s)	0.00E+00	0.00E+00	0.00E+00	3.35E-01
25	NaCl(1)	2.09E-01	3.21E-01	3.34E-01	0.00E+00
26	Na2CO3(2)	0.00E+00	0.00E+00	5.23E-07	2.35E-07

Table 2. Equilibrium of Simulated Flue Gas - NaCl - SO2 System At One Atm

Number	Compound	Mole Fraction			
		Temperature °C			
		1500	1300	1100	900
1	CO	2.16E-06	6.17E-08	5.33E-10	5.54E-13
2	CO2	6.82E-02	6.69E-02	6.67E-02	6.67E-02
3	Cl	1.19E-05	4.22E-06	8.81E-07	8.78E-08
4	ClO	4.52E-08	2.29E-08	7.10E-09	1.22E-09
5	Cl2	5.34E-08	1.72E-07	5.11E-07	2.13E-06
6	HCl	4.92E-04	5.86E-04	6.08E-04	6.06E-04
7	HOCl	2.40E-08	2.50E-08	1.99E-08	1.33E-08
8	HO2	3.64E-08	8.11E-09	1.03E-09	5.25E-11
9	H2	2.67E-07	1.12E-08	1.69E-10	4.09E-13
10	H2O	2.18E-02	2.14E-02	2.13E-02	2.13E-02
11	NO	3.10E-04	9.83E-05	2.11E-05	2.29E-06
12	NO2	5.60E-07	3.85E-07	2.20E-07	9.74E-08
13	N2	5.71E-01	5.60E-01	5.59E-01	5.59E-01
14	N2O	1.83E-08	6.72E-09	1.65E-09	2.19E-10

Table 2. Continued.....

15	Na	2.39E-06	3.34E-09	6.64E-13	1.58E-18
16	NaCl	8.67E-02	8.50E-03	3.91E-04	2.21E-06
17	NaO	9.82E-08	1.98E-10	5.95E-14	2.54E-19
18	NaOH	1.35E-04	1.90E-06	7.93E-09	1.54E-12
19	Na2Cl2	2.31E-02	2.89E-03	1.71E-04	6.72E-07
20	Na2SO4	2.63E-05	7.71E-07	5.71E-09	2.56E-12
21	O	4.87E-07	1.95E-08	2.73E-10	5.88E-13
22	OH	1.93E-05	2.46E-06	1.59E-07	3.10E-09
23	O2	1.85E-02	1.82E-02	1.82E-02	1.82E-02
24	SO2	1.28E-04	1.19E-05	2.88E-07	2.52E-09
25	SO3	7.37E-07	2.40E-07	2.98E-08	2.80E-09
26	NaCl(s)	0.00E+00	0.00E+00	0.00E+00	3.34E-01
27	NaCl(l)	2.09E-01	3.21E-01	3.33E-01	0.00E+00
28	Na2SO4(i)	0.00E+00	0.00E+00	3.05E-04	3.05E-04
29	Na2SO4(l)	1.57E-04	2.90E-04	0.00E+00	0.00E+00

Table 3. Initial Reactants Feed In The System

Compound	Weight (%)	State	Temperature (K)
N_2	80	gas	298.15
O_2	3	gas	298.15
CO_2	15	gas	298.15
H_2O	2	gas	298.15
NaCl	100	solid	298.15

Table 4. Species Being Considered In The Equilibrium In a Simulated Flue Gas - NaCl System At One Atm

```
THERMO
REACTANTS
N   2.0000        0.0000      0.0000      0.0000      0.0000    80.000000      0.00 G   298.150     0
O   2.0000        0.0000      0.0000      0.0000      0.0000     3.000000      0.00 G   298.150     0
C   1.0000  O     2.0000      0.0000      0.0000      0.0000    15.000000      0.00 G   298.150     0
H   2.0000  O     1.0000      0.0000      0.0000      0.0000     2.000000      0.00 G   298.150     0
NA  1.0000  CL    1.0000      0.0000      0.0000      0.0000   100.000000      0.00 S   298.150     F

OSPECIES BEING CONSIDERED IN THIS SYSTEM
 J 3/78  C            J12/69  CCL          J12/68  CCL2         J 6/70  CCL3         P12/81  CCL4
 J12/67  CH           RUS 79  CHCL         P 6/81  CHCL3        J12/72  CH2          P12/81  CH2CL2
 J 3/61  FORMALDEHYDE L 4/85  FORMIC ACID  J 6/69  CH3          P12/81  CH3CL        L 9/85  HYDROXYMETHYLENE
 L 9/85  METHYLOXIDE  L 5/84  CH4          L 9/85  METHANOL     J 6/69  CN           J12/70  NCN RAD
 J 6/66  CNN RAD      J 9/65  CO           J12/65  COCL         J 6/61  COCL2        J 9/65  CO2
 J12/69  C2           J12/68  C2CL2        L10/87  C2CL4        L10/87  C2CL6        J 3/67  C2H RAD
 RUS 79  C2HCL        J 3/61  ACETYLENE    8UR 84  KETENE       8UR 84  C2H3 RAD     8UR 84  METHYL CYANIDE
 8UR 84  CH3CO RAD    8UR 84  CH2CHO RAD   L 4/85  ETHYLENE     8UR 84  ACETALDEHYDE L 4/85  ACETIC ACID
 L 4/85  (FORMIC ACID)2 P10/83 ETHYL RAD    8UR 84  ETHYL OXIDE RAD L 5/84 ETHANE     8UR 84  AZOMETHANE
 8UR 84  ETHANOL      8UR 84  DIMETHYL ETHER J 3/67  CNC RAD     J 3/61  CYANOGEN     J 9/66  CCO RAD
 J12/69  C3           0B6/61  C3H3 RAD     8UR 84  CYCLOPROPENE 8UR 84  PROPYNE      8UR 84  ALLENE
 8UR 84  C3H5 RAD     8UR 84  CYCLOPROPANE L 4/85  PROPYLENE    L 9/85  PROPYLENE OXIDE L 9/85  I-PROPYL RAD
 L 9/85  N-PROPYL RAD L 4/85  PROPANE      L 1/84  1-PROPANOL    J 6/68  CARBON SUBOXIDE J12/69  C4
 8UR 84  BUTADIYNE    8UR 84  BUTAN-1EN-3YN P10/85  CYCLOBUTADIENE 8UR 84 2-BUTYNE    P 4/84  1,3-BUTADIENE
 8UR 84  2-BUTENE TRANS 8UR 84 2-BUTENE CIS 8UR 84  ISOBUTENE    8UR 84  1-BUTENE     L 4/85  (ACETIC ACID)2
 L 9/85  S-BUTYL RAD  P10/83  N-BUTYL RAD  L 9/85  T-BUTYL RAD  L 4/85  ISOBUTANE    L 4/85  N-BUTANE
 J 3/61  CARBON SUBNITRID J12/69 C5        P10/85  CYCLOPENTADIENE P12/52 CYCLOPENTANE P12/52 1-PENTENE
 P10/83  N-PENTYL RAD L 5/87  T-PENTYL RAD P10/85  CH3C(CH3)2CH3 P10/85 PENTANE     P10/85  ISOPENTANE
 8UR 84  HEXATRIYNE   L12/84  PHENYL RAD   L12/84  PHENOXY RAD  L12/84  BENZENE      L12/84  PHENOL
 8UR 84  CYCLOHEXENE  P10/83  N-HEXYL RAD  L 3/86  BENZALDEHYDE P10/84  TOLUENE      L 6/87  CRESOL
 P12/52  1-HEPTENE    P10/83  N-HEPTYL RAD P 4/81  N-HEPTANE    P12/52  1-OCTENE     P10/83  N-OCTYL RAD
 P 4/85  OCTANE       P 4/85  ISO-OCTANE   P10/83  N-NONYL RAD  8UR 84  NAPTHLENE    8UR 84  AZULENE
 P10/83  N-DECYL RAD  L12/84  O-BIPHENYL RAD L12/84 BIPHENYL    L 6/88  JET-A(G)     L 6/87  BIBENZYL
 J 6/72  CL           J 6/66  CLCN         J 6/61  CLO          J 3/61  CLO2         J 9/65  CL2
 J12/65  CL2O         J 3/77  H            L12/69  HCN          J12/70  HCO RAD      J 9/64  HCL
 J12/70  HNCO         RUS 78  HNO          RUS 78  HNO2         RUS 78  HNO3         J 3/79  HOCL
 J 9/78  HO2          J 3/77  H2           J12/65  H2N2         J 3/79  H2O          L 3/85  H2O2
 J 3/77  N            J12/70  NCO          RUS 78  NH           RUS 78  NH2          J 6/77  NH3
 RUS 78  NH2OH        RUS 78  NO           RUS 78  NOCL         RUS 78  NO2          RUS 78  NO2CL
 J12/64  NO3          J 3/77  N2           RUS 78  N2H2         RUS 78  NH2NO2       RUS 78  N2H4
 RUS 78  N2O          RUS 78  N2O3         RUS 78  N2O4         RUS 78  N2O5         RUS 78  N3
 RUS 78  N3H          J 6/62  NA           J3/66   NACN         J12/64  NACL         J 3/63  NAH
 J12/67  NAO          J12/70  NAOH         J 6/62  NA2          J3/66   NA2C2N2      J12/64  NA2CL2
 K10/74  NA2O         J12/70  NA2O2H2      J 3/77  O            J 6/77  OH           J 3/77  O2
 J 6/61  O3           J 3/78  C(GR)        P10/80  BENZENE(L)   P10/80  TOLUENE(L)   P10/80  OCTANE(L)
 L 6/88  JET-A(L)     L 3/81  H2O(S)       J 3/79  H2O(L)       8AR73   NH4CL(A)     8AR73   NH4CL(B)
 J 6/62  NA(S)        J 6/62  NA(L)        J 3/66  NACN(S)      J 3/66  NACN(L)      J 9/64  NACL(S)
 J 9/64  NACL(L)      J12/70  NAOH(A)      J12/70  NAOH(L)      J 6/63  NAO2(S)      J 3/66  NA2CO3(1)
 J 3/66  NA2CO3(2)    J 3/66  NA2CO3(L)    J 6/68  NA2O(C)      J 6/68  NA2O(A)      J 6/68  NA2O(L)
 J 6/68  NA2O2(A)     J 6/68  NA2O2(B)
```

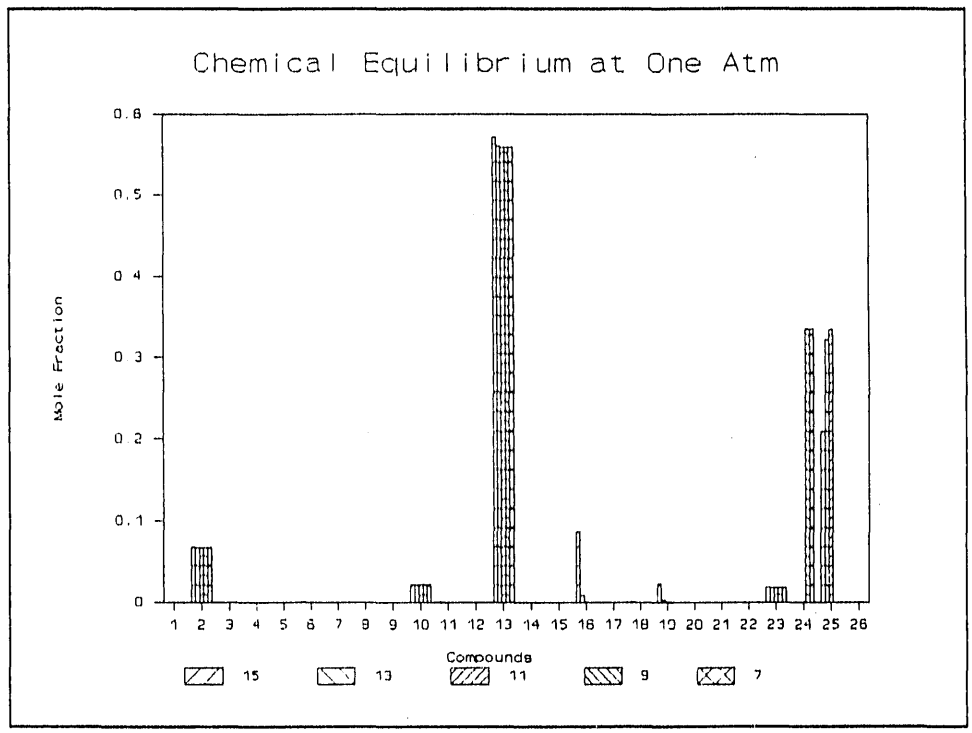

Temperature: Legend Number * 100 °C

Figure 3. Chemical Equilibrium at Different Temperature

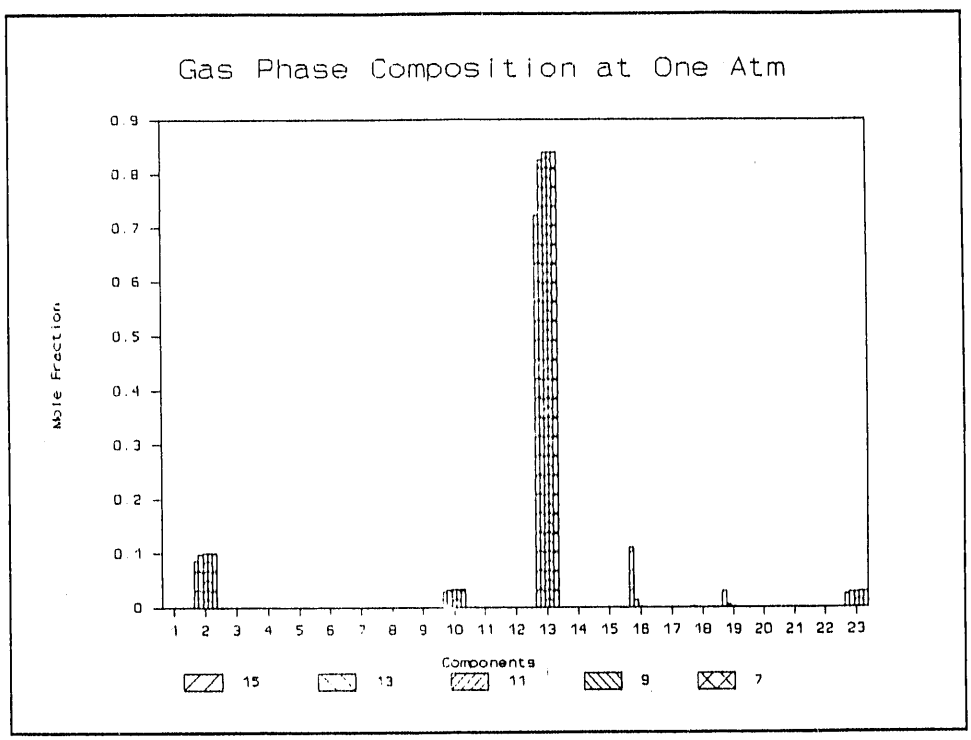

Temperature: Legend Number * 100 °C

Figure 4. Gas Phase Composition at Equilibrium

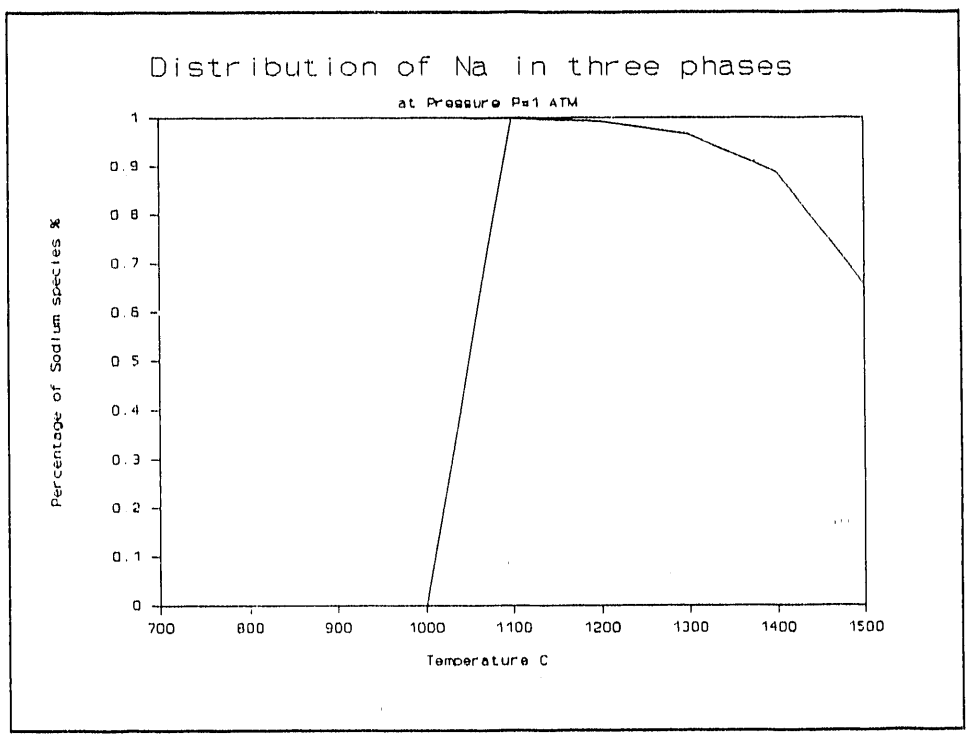

1. Gas Phase; 2. Liquid Phase; 3. Gas Phase

Figure 5. The Temperature Effect On The Distribution of Sodiun Species In Different Phases

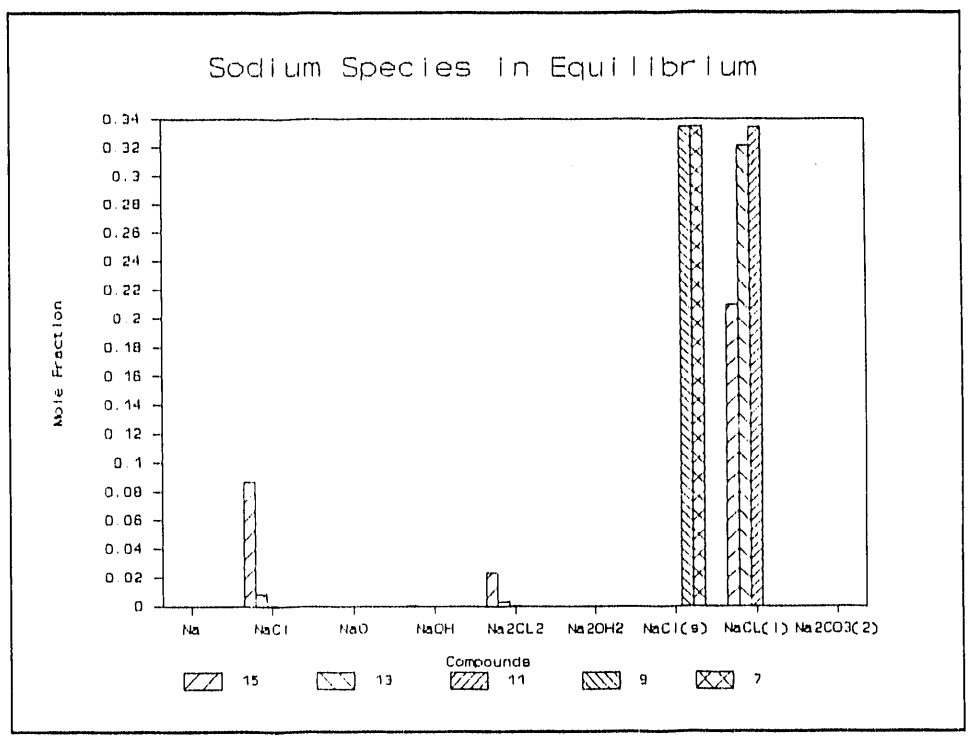

Temperature: Legends Number * 100 °C

Figure 6. Sodium Species Distribution AT One Atm Pressure

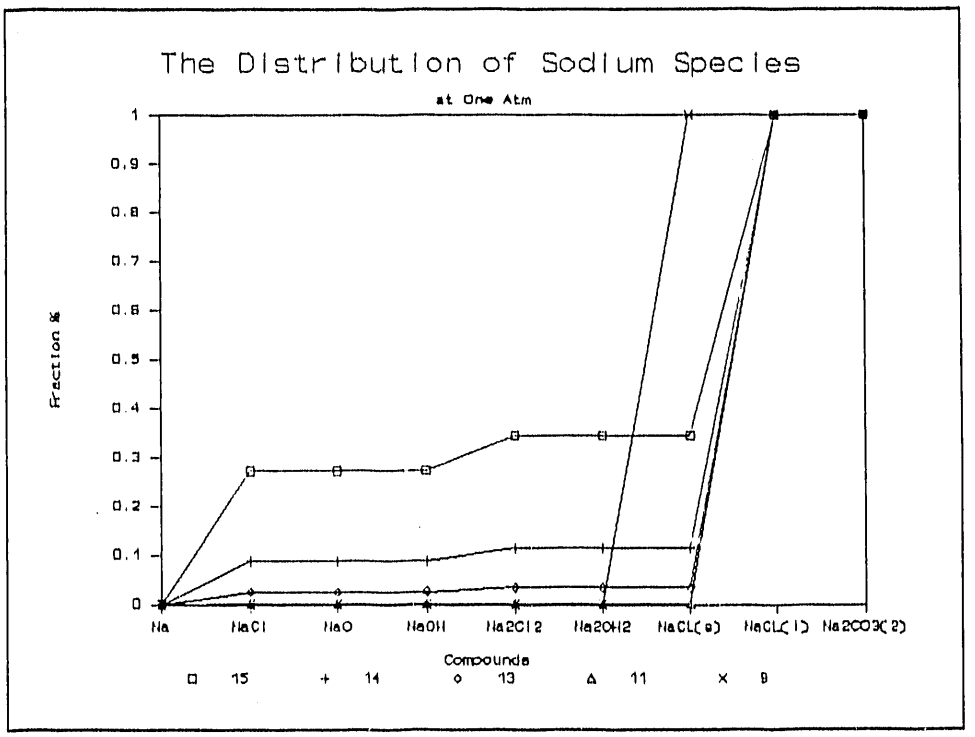

Temperature: Symbol Number *100 °C

Figure 7. The Integrated Form Of Sodium Distribution

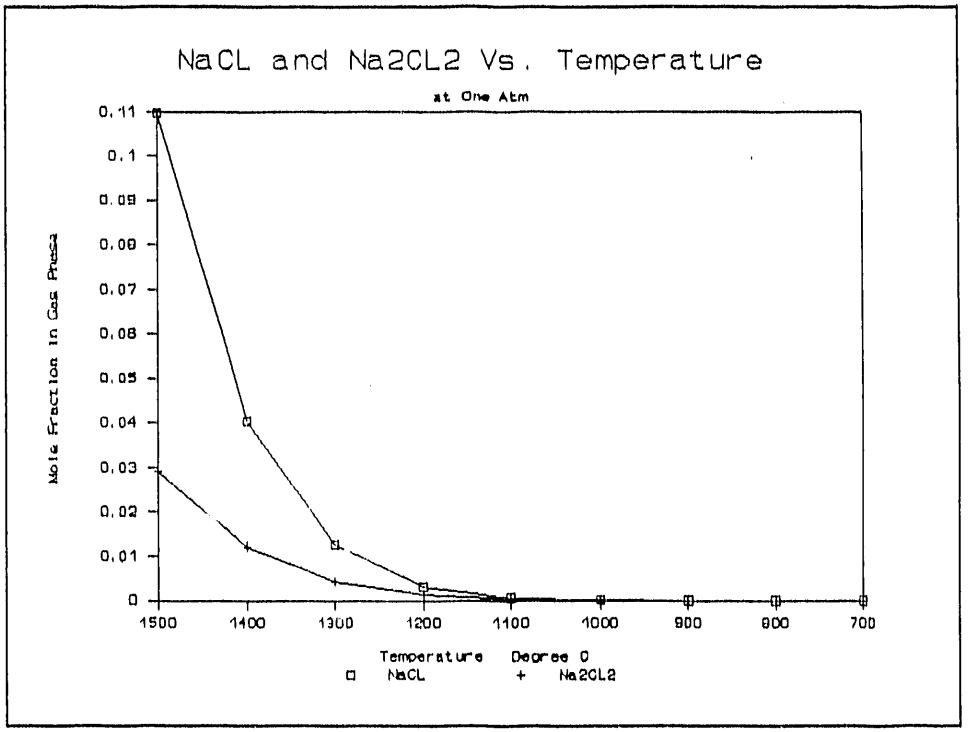

Figure 8. The Effect Of Temperature On NaCl And Na_2Cl_2

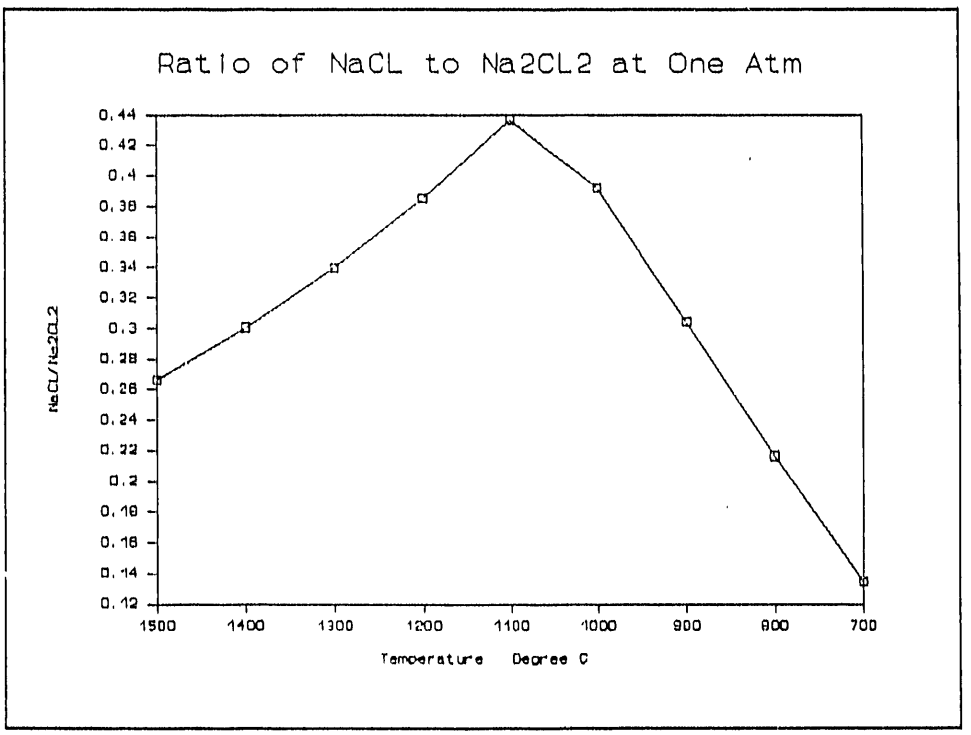

Figure 9. The Effect Of Temperature On Na_2Cl_2/NaCL

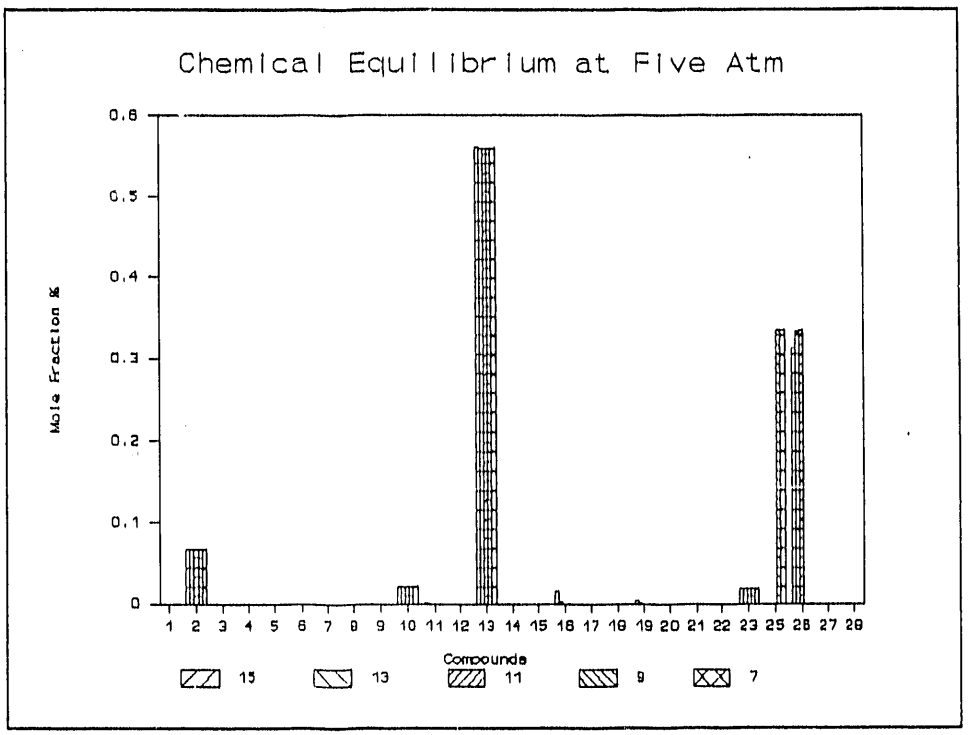

Temperature: Legend Number * 100 °C

Figure 10. The Equilibrium Composition At Five Atm

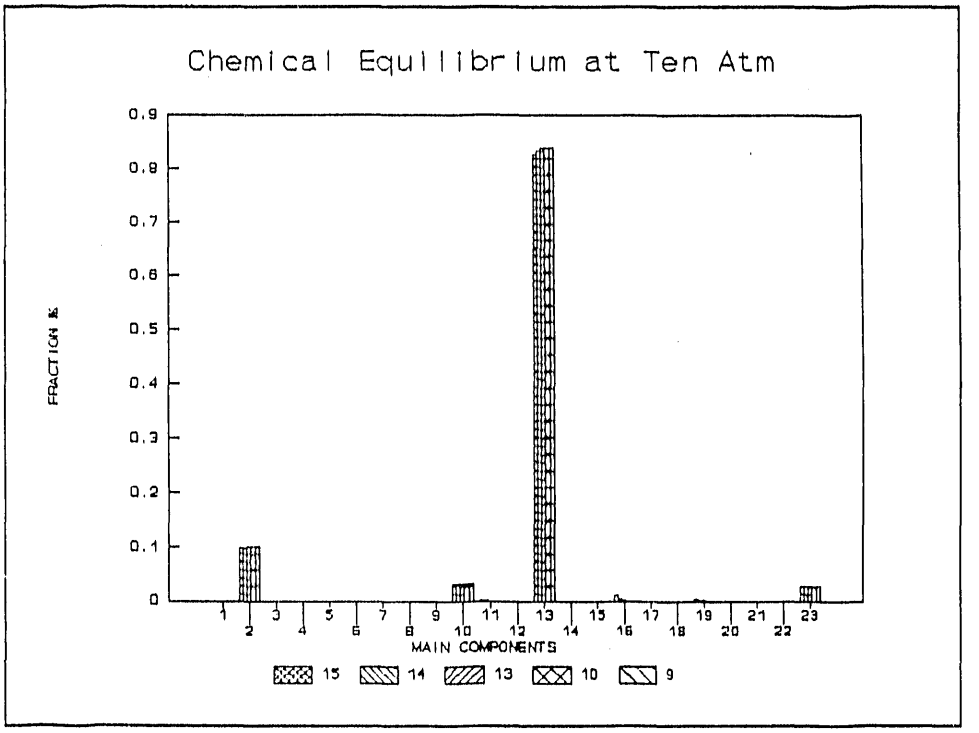

Temperature: Legend * 100 °C

Figure 11. Equilibrium Calculation At Tem Atm

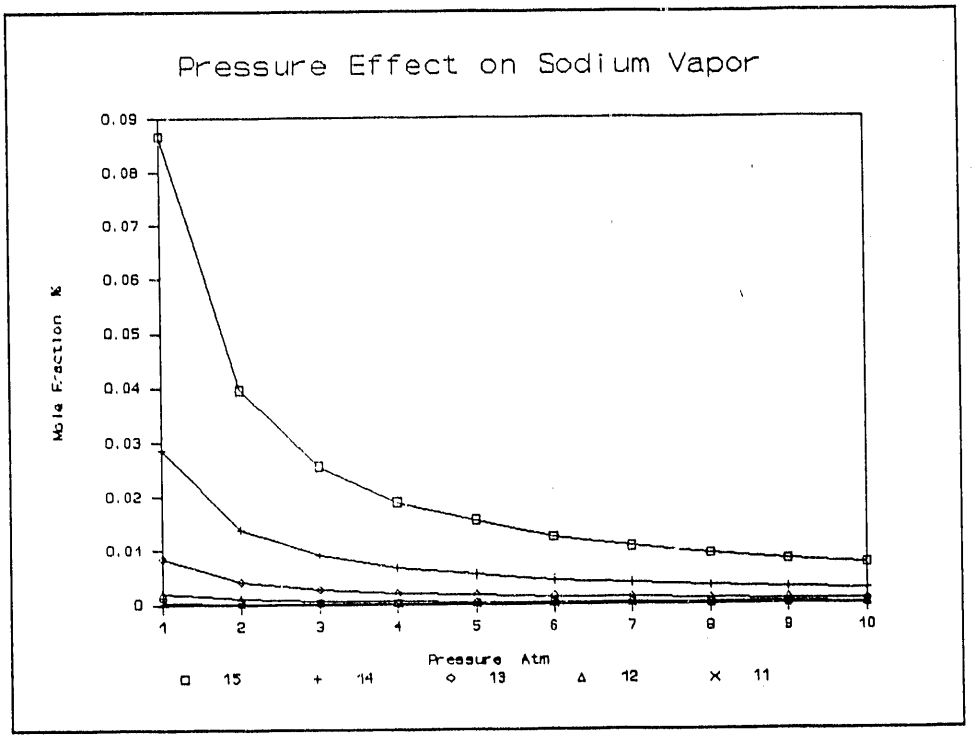

Temperature: Symbol Number * 100 °C

Figure 12. Pressure Effect On NaCl Vapor Generation

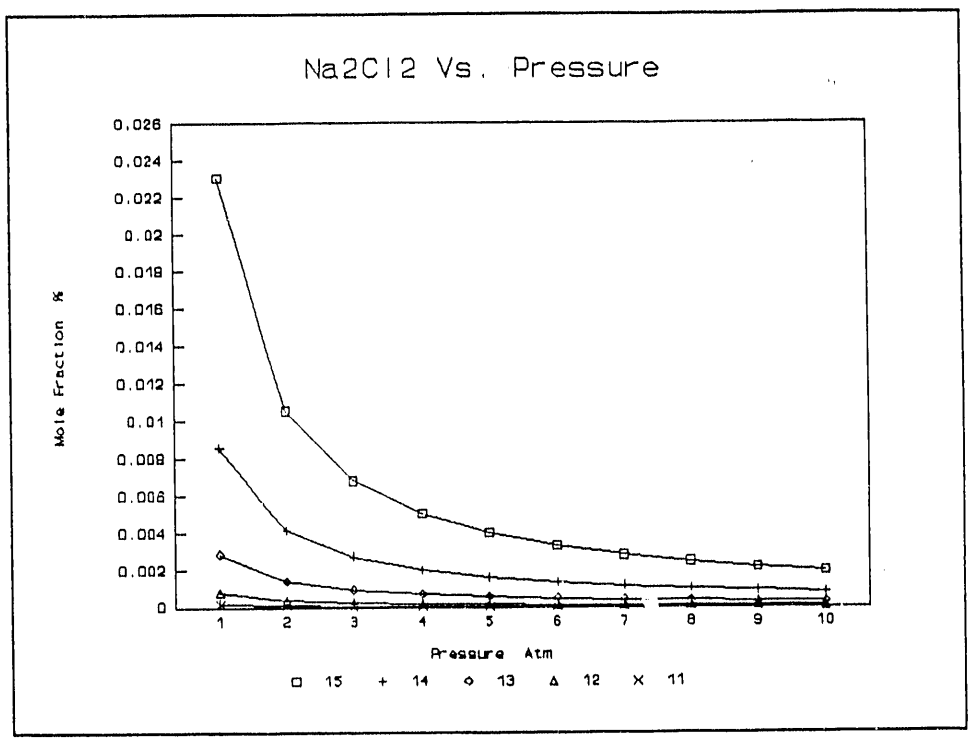

Temperature: Symbol Number * 100 °C

Figure 13. The Effect Of Pressure On the Formation of Na_2Cl_2

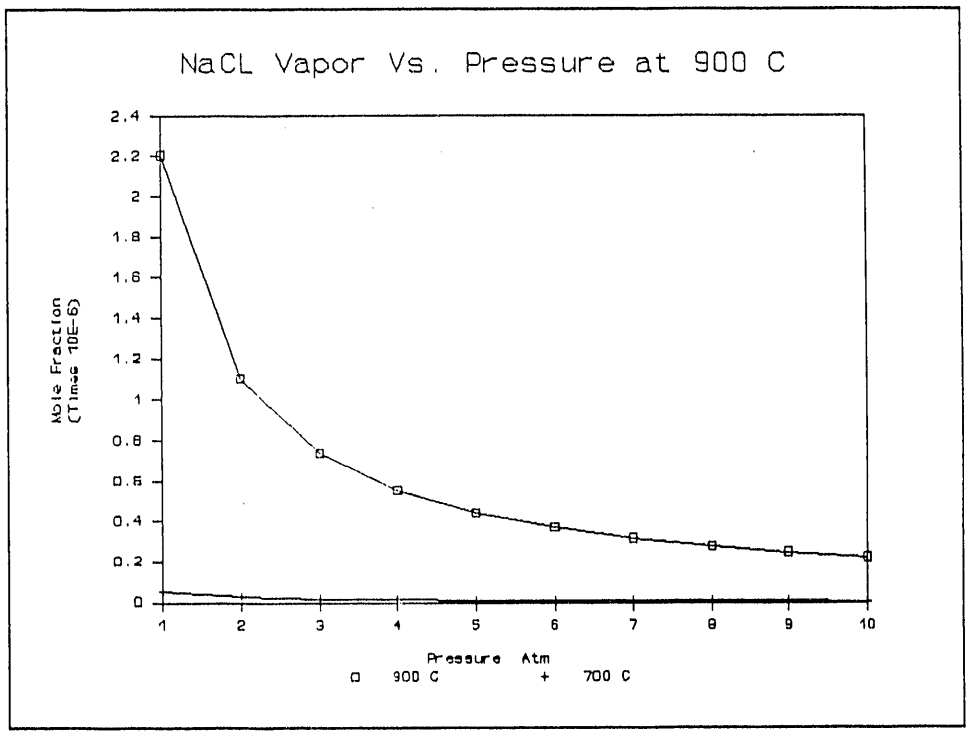

Figure 14. The Effect Of Pressure On NaCl At 900 °C

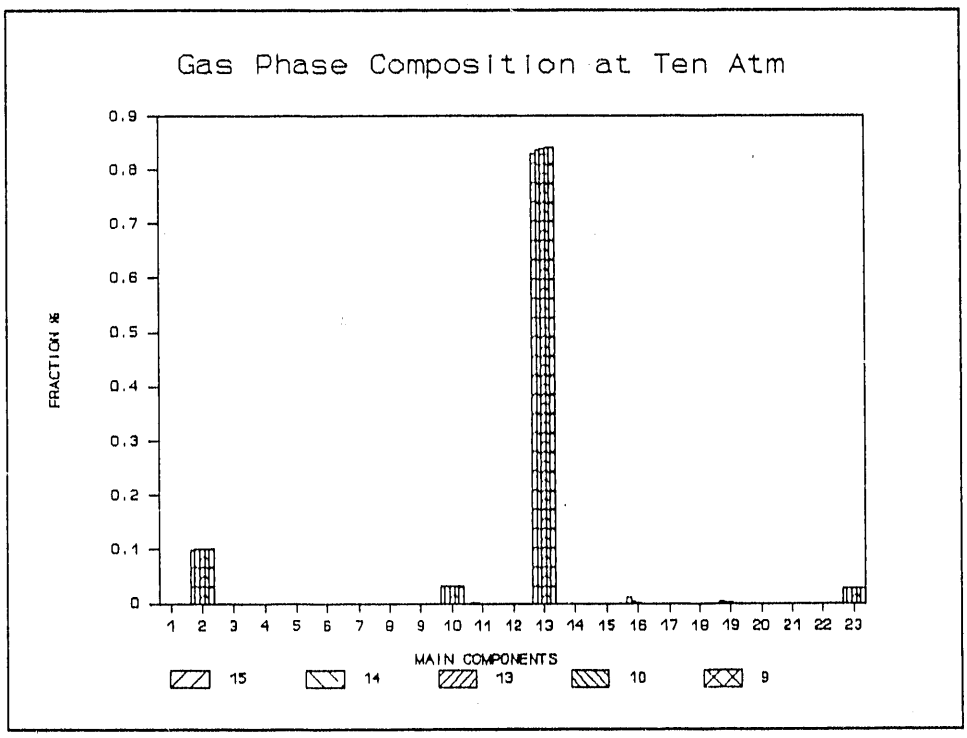

Temperature: Legend * 100 °C

Figure 15. Gas Phase Composition At Equilibrium At Ten Atm

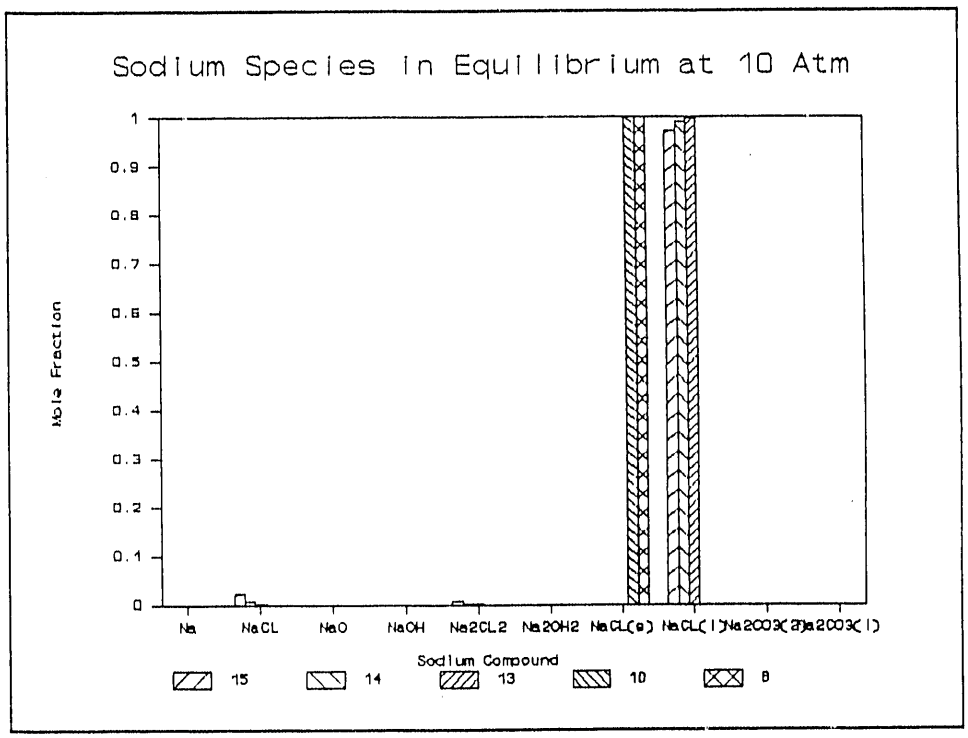

Temperature: Legend Number * 100 °C

Figure 16. Temperature Effect On Sodium Species Distribution

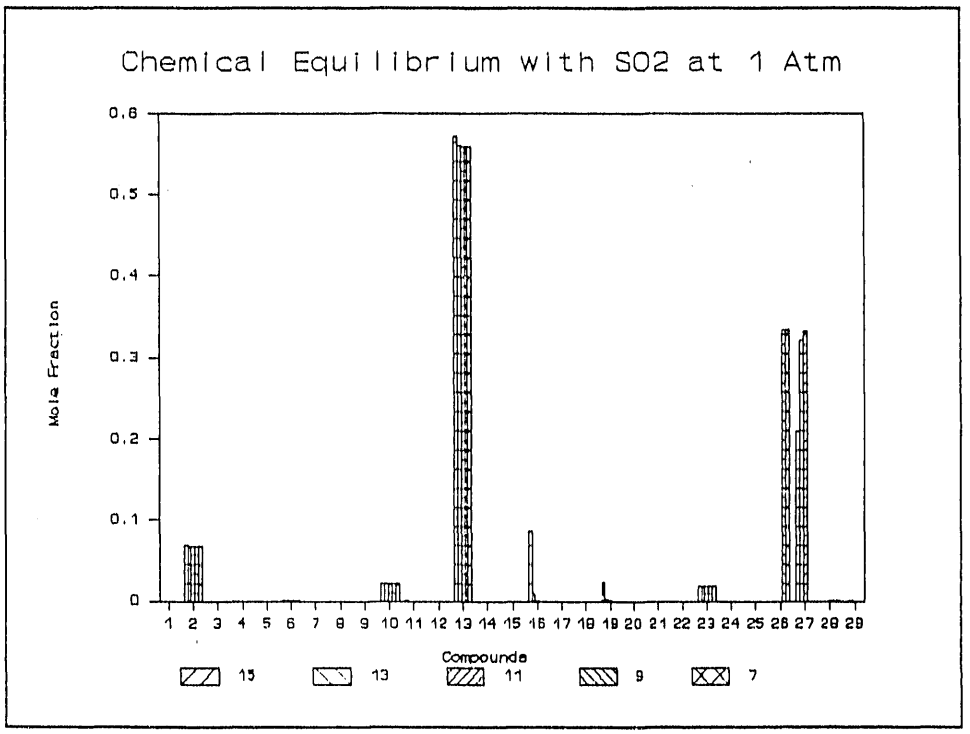

Temperature: Legend Number * 100 °C

Figure 17. Chemical Equilibrium At One Atm With SO_2

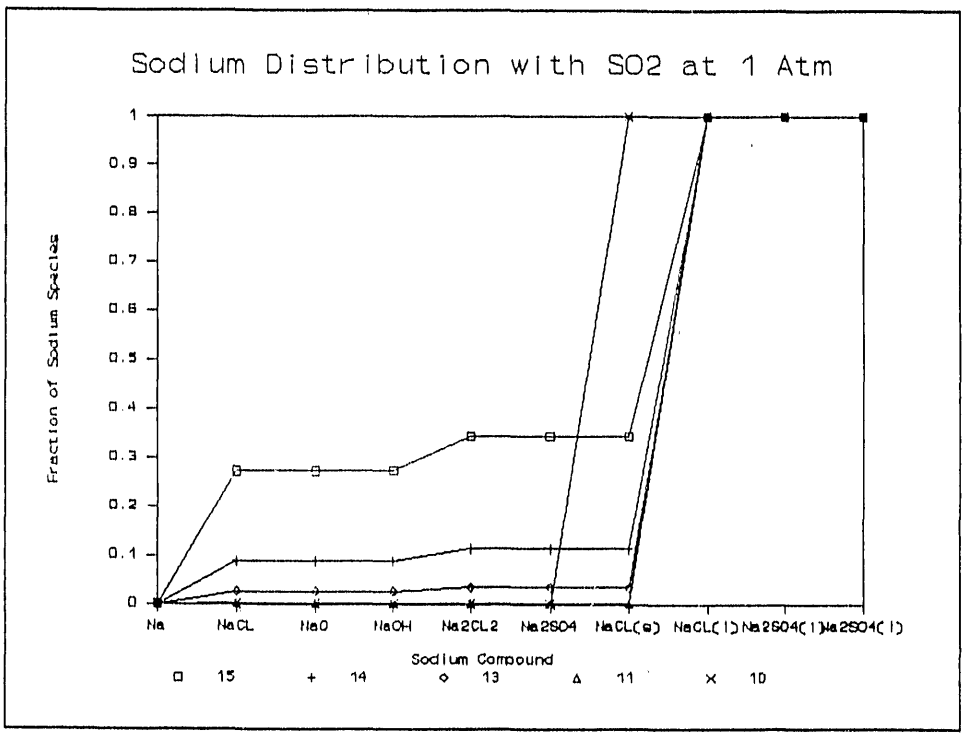

Temperature: Symbol Number * 100 °C

Figure 18. The Equilibrium Distribution Of Sodium Species

END

DATE
FILMED
4/7/92

I